A phenomenological drag law in blast-soil interaction

Xiaoling Tong

Center for Advanced Vehicular Systems, Mississippi State University

Simcenter/CAVS, 2 Research Blvd, Starkville, MS 39759, USA

Email: xltong@cavs.msstate.edu

Phone number: 001-662-3253048

Fax number: 001-662-3257692

Edward Luke

Department of Computer Science, Mississippi State University

Butler Hall, Box 9637

Mississippi State University, MS 39762, USA

Michael Remotigue

Center for Advanced Vehicular Systems, Mississippi State University

Jian Kang

TARDEC, Warren, Michigan

January 16, 2013

Report Documentation Page

Form Approved
OMB No. 0704-0188

1. REPORT DATE	2. REPORT TYPE	3. DATES COVERED
16 JAN 2013	**Journal Article**	**16-01-2013 to 16-01-2013**

4. TITLE AND SUBTITLE
A phenomenological drag law in blast-soil interaction

5a. CONTRACT NUMBER
W56HZV08C0236

5b. GRANT NUMBER

5c. PROGRAM ELEMENT NUMBER

6. AUTHOR(S)
Xiaoling Tong; Edward Luke; Michael Remotigue; Jian Kang

5d. PROJECT NUMBER

5e. TASK NUMBER

5f. WORK UNIT NUMBER

7. PERFORMING ORGANIZATION NAME(S) AND ADDRESS(ES)
U.S. Army TARDEC ,6501 E.11 Mile Rd,Warren,MI,48397-5000

8. PERFORMING ORGANIZATION REPORT NUMBER
#23604

9. SPONSORING/MONITORING AGENCY NAME(S) AND ADDRESS(ES)
U.S. Army TARDEC, 6501 E.11 Mile Rd, Warren, MI, 48397-5000

10. SPONSOR/MONITOR'S ACRONYM(S)
TARDEC

11. SPONSOR/MONITOR'S REPORT NUMBER(S)
#23604

12. DISTRIBUTION/AVAILABILITY STATEMENT
Approved for public release; distribution unlimited

13. SUPPLEMENTARY NOTES

14. ABSTRACT

One challenge associated with the simulation of buried detonations involves the treatment of the multiphase ow phenomena related to the soil. At the moment when the soil shatters" into a dense particulate cloud with detonation products escaping through the soil particles, the continuum model that assumes a single velocity shared by the blast gas and the soil at any given point no longer holds. Instead momentum coupling between the two phases has to be modeled. One characteristic at the stage of soil breaking is that the soil fragments packed in a tight con guration under large pressure provide signi cant blockage e ect characterized by large particle volume fractions. Unfortunately, traditional drag laws do not address the momentum coupling between gas and solid phase under the condition of particle high volume fraction in high speed blast ows. In order to develop a phenomenological drag model to characterize the momentum coupling between the detonation gas and soil fragments when the soil initially breaks into a dense particulate cloud we conducted a series of numerical simulations on the scale of soil fragments by only considering a small region occupied by a mixture of blast gas and soil fragments (so-called particle-scale simulations). A drag database was constructed based on the drag force collected from the particle- scale simulations under the conditions of various soil volume fractions and particle sizes. A new drag law was developed using data regression technique to characterize the dependency of the drag force exerted on particles as a function of particle volume fraction and Reynolds number based on particle size. The proposed drag law provides satisfactory representations of the simulation data and converge to traditional drag model for isolated particles when the particle volume fraction approaches to zero. Finally, we applied the new phenomenological drag law in the simulations of buried detonation at the stage of soil breaking, and compared the results with the ones from continuum model in which the gas and the soil are assumed moving at the same speed.

15. SUBJECT TERMS

Drag law, Computational fluid dynamics, Dense particulate flow, Blast wave, Data regression

16. SECURITY CLASSIFICATION OF:			17. LIMITATION OF ABSTRACT	18. NUMBER OF PAGES	19a. NAME OF RESPONSIBLE PERSON
a. REPORT	b. ABSTRACT	c. THIS PAGE			
unclassified	**unclassified**	**unclassified**	**Public Release**	**24**	

Abstract

One challenge associated with the simulation of buried detonations involves the treatment of the multiphase flow phenomena related to the soil. At the moment when the soil "shatters" into a dense particulate cloud with detonation products escaping through the soil particles, the continuum model that assumes a single velocity shared by the blast gas and the soil at any given point no longer holds. Instead momentum coupling between the two phases has to be modeled. One characteristic at the stage of soil breaking is that the soil fragments packed in a tight configuration under large pressure provide significant blockage effect characterized by large particle volume fractions. Unfortunately, traditional drag laws do not address the momentum coupling between gas and solid phase under the condition of particle high volume fraction in high speed blast flows. In order to develop a phenomenological drag model to characterize the momentum coupling between the detonation gas and soil fragments when the soil initially breaks into a dense particulate cloud, we conducted a series of numerical simulations on the scale of soil fragments by only considering a small region occupied by a mixture of blast gas and soil fragments (so-called particle-scale simulations). A drag database was constructed based on the drag force collected from the particle-scale simulations under the conditions of various soil volume fractions and particle sizes. A new drag law was developed using data regression technique to characterize the dependency of the drag force exerted on particles as a function of particle volume fraction and Reynolds number based on particle size. The proposed drag law provides satisfactory representations of the simulation data, and converge to traditional drag model for isolated particles when the particle volume fraction approaches to zero. Finally, we applied the new phenomenological drag law in the simulations of buried detonation at the stage of soil breaking, and compared the results with the ones from continuum model in which the gas and the soil are assumed moving at the same speed.

KEY WORD: Drag law, Computational fluid dynamics, Dense particulate flow, Blast wave, Data regression

1 Introduction

In CFD simulations of explosive blast wave traveling through broken soil fragments in the case of buried detonations, while the behavior of the blast wave is simulated in the regular flow solver, the small scale and large number of soil fragments make it impractical to simulate the behavior of soil particles directly in the flow solver. Therefore, multiphase coupling effects between solid phase (soil fragments) and gas phase (detonation gas) need to be modeled. The momentum transfer between two phases is one of essential coupling terms to be considered since it is critical for the accurate modeling of blast loading on the target. One challenge associated with momentum transfer between two phases for buried detonation is how to correctly model the behavior of the soil that surrounds the expanding cloud of detonation products. At the moment when soil "shatters", or breaks into a cloud of particulates, the continuum model that assumes a single velocity shared by the gas and soil is no longer appropriate. Instead, a drag model that describes the functional dependency of the drag force exerted on soil is needed. One characteristic at the initial stage of soil breaking is that the soil fragments are packed in a tight configuration under large pressure, providing a significant blockage effect characterized by large volume fractions.

There have been significant amount of effort on investigating particle drag models in past decades, ranging from theoretical work in Stokes flow to empirical formulations [Crowe, 1998]. Traditional multiphase models normally consider a dispersed phase where drag laws are developed assuming that each particle is isolated. As the number of particles increases in a fixed space, two effects become important: 1) particle drag laws can no longer assume isolated particles as one particle will be in the viscous wake of other particles, and 2) a non-negligible amount of volume occupying by the particles will cause non-trivial blockage effects in the fluid phase. Collectively, these two effects are considered as large volume fraction effects, and they only occur when particle volume fraction becomes significant (greater than 1%). However, there is little information available on the drag of particles in dense particle clouds, with mostly commonly mentioned work coming from the sedimentation and fluidization

studies [Gidaspow, 1994], which is not applicable to the high speed blast flows. Properly capturing large volume fraction effects is required to reliably describe the dense particulate flows in blast wave that occur in buried detonations. However, current available models make no attempt to capture these effects. The goal of this study is to develop appropriate phenomenological drag laws with inclusion of the effects of large volume fractions to correctly model multiphase effect in buried detonation simulations at the stage of soil failing. In this study, we carried out the numerical simulations in the scale of soil fragment by zooming into the a small region occupied by the mixture of soil fragments and the gas, and the drag force acting on each soil fragments was computed in this particle-scale simulation. The database that is a collection of the drag force from a series of particle-scale simulations under various particle volume fractions and sizes was established. Then the drag laws were obtained by analyzing the data from the database. In the following, the first step of particle-scale numerical simulations including geometry modeling and mesh generation will be described, followed by the presentation of the simulation set-up and results. The database of collected drag force and the drag laws based on the regression of the database will be discussed in the end.

2 Geometry model and mesh generation

We wish to simulate the coupling effects between gas and particles under high volume fractions in the moments associated with soil failure. The geometry of the particles in this circumstance cannot be approximated as spherical objects due to the high packing. In order to obtain very large volume fractions, we need to construct particle geometries such that the particles can be expanded and returned to their original continuous state. To accomplish this task, we modeled the particles by constructing a Voronoi graph about a random set of seed points. The Voronoi graph mimics cleaves that form between particles,and expansion of the the Voronoi graph creates gaps where the passage of gas was modeled. The Voronoi diagram subdivides a region into a set of Voronoi cells, each of which is associated with a specific “seed” point. A Voronoi cell has the property that all points contained within the cell are

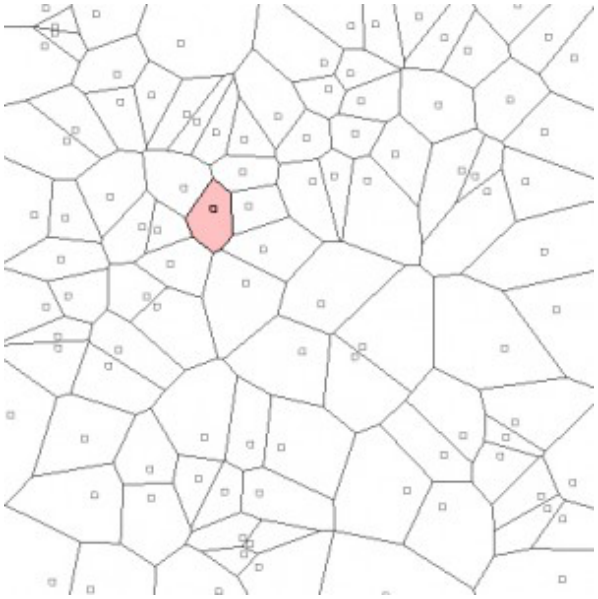

Figure 1: Two-dimensional represnetation of Voronoi diagram (image from http://www.donhavey.com/blog/tutorials/tutorial-7-voronoi-diagrams/).

closer to its seed point that to all other seed points in the domain. Figure 1 shows a Voronoi diagram for a planar set of randomly generated points. The "borders" of each cell have equal distance between the seed points of adjacent cells. This creates convex regions that can be organized or grouped as soil fragments. In order to reduce the size of the computational domain needed to simulate, the Voronoi graph was constructed to be periodic. This approach accommodates creating geometry of arbitrarily large particle volume fractions.

Four pieces of information were used to create the simulated particle formation, namely particle centers (random points), Voronoi points, Voronoi neighbors around the Voronoi points, and the Voronoi points for each Voronoi region. The particles were assembled by isolating the neighbor map for each Voronoi region and only the regions with positive neighbors and overlapped with the unit cubes were considered. The cube and the particles were then displaced/expanded from the center of the unit

cube like expanding the universe to create various volume fraction. The particle faces were then formed by traversing the particle neighbor map and only considering points that lie within a plane to form a closed loop that represents the surface of the particle. The faces were then intersected with Y and Z planes of the cubes. Any parts that were not fully enclosed in the cube were trimmed. The functionality of the SolidMesh library [Gaither et al., 2000] was used to assemble the geometric description and perform any necessary geometric operations. The resultant geometry was assembled into a solid modeling representation and output as a SolidMesh save state which can be read into SolidMesh for mesh generation.

There are competing concerns that must be balanced in building geometry model. We would like to have as many soil fragments as possible to better approximate an actual particle cloud; however, we cannot afford to have meshes that contain a large number of cells due to computational cost. Based on some preliminary studies, we determined that having 10 soil fragments per unit volume (with overall number of fragments at about 40) and utilizing periodic boundaries provide a good compromise between computational cost and the ability to capture true multiphase effects. Figure 2 shows the fluid portion of the periodic cube of particulate grain. In this figure, the outer faces on X direction are placed a few unit away from the expanding unit cube to decrease the boundary effect for the flow simulations. In this model, 10 random points in one unit volume are generated (with total of 34 random points) and expansion rate is 1.25 which corresponds to particle volume fraction of 51.2%. Only those particles that are fully enclosed in the cube and that intersected the Y and Z planes were considered in the simulations. The particles with surrounding faces turned off are shown in figure 3.

3 Numerical Simulations

When the flow is dilute where the particle volume fraction is small, the drag coefficient exerted on the isolated particle is a function of Reynolds number based on particle size and the relative velocity between two phases, according to traditional drag laws [Clift and Gauvin, 1970]. Thus the particle

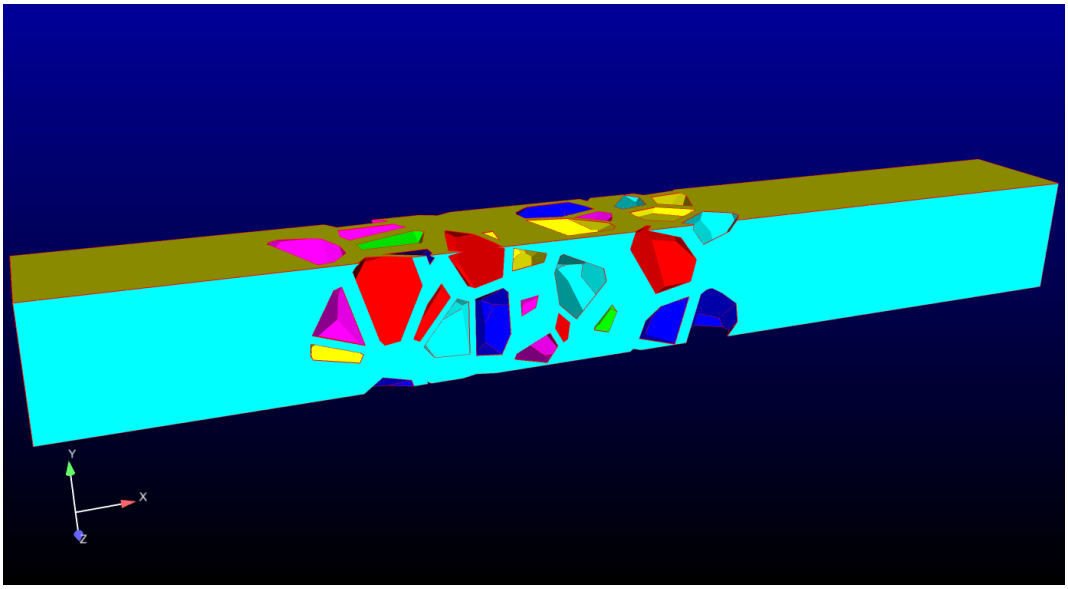

Figure 2: Outer face of periodic cube of particle cloud

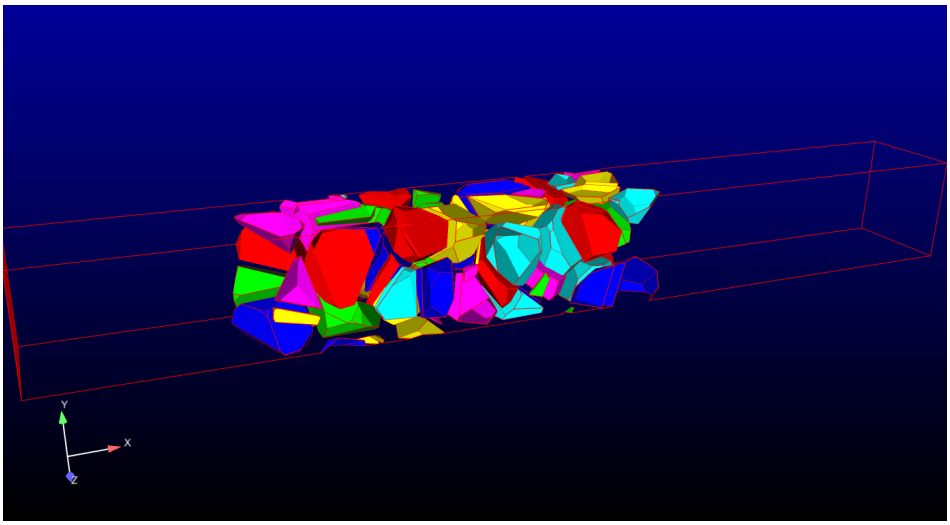

Figure 3: The underlying particle cloud

size plays a dominant role in the cases of low particle volume fraction where the viscous effects are important. When the particles are densely packed in the flow field, the drag between particles and the gas mainly comes from inviscid nature of the flow, and the particle volume fraction plays a significant role. In order to evaluate the importance of soil size and soil volume fraction on momentum transfer between soil fragments and high pressure detonation gas, which leads to a phenomenological drag model of blast gases flowing through particles, a series of cases with high pressure flows passing through a number of soil fragment pieces with different particle sizes and volume fractions was simulated in the small zoomed-in region of the domain (so-called particle-scale simulations). About 40 pieces of soil fragments existed in the simulation domain. There were six different expansion ratios of soil fragment centroids, namely 1.2, 1.25, 1.5, 2, 5 and 10, which corresponded to soil volume fractions of 57.8%, 51.2%, 29.6%, 12.5%, 8% and 0.1%. This range of volume fractions covers the cases with densely packed soil blocks to the situations with dilutely distributed soils. Figures 4 and 5 show the configurations of soil fragments with highest and lowest particle volume fractions in our particle-scale simulations. Under each volume fraction, five different soil sizes are evaluated, which is on the order of $0.1mm$, $0.3mm$, $1mm$, $3mm$ and $1cm$. The different soil size is achieved by setting corresponding reference length in the simulations. The computational domain is a rectangular box with periodic boundary conditions imposed at four boundaries surrounding the soil fragments in both Y and Z directions simulating an infinite field of debris. The flow direction is along the X axis and we provided a buffer region ahead of and behind the flow so that the flow could equilibrate before reaching the boundaries.

In the case of blast simulations, the gas flow and particles are in complete momentum equilibrium and hence have the same velocity at the moment when particle cloud is formed. The gas is able to pass through gaps between the soil fragments. Note that while the gas and particles may be traveling at supersonic speed, the relative velocities between the two materials is subsonic at the moment of soil failure. Thus the numerical simulations focus on flow through the particulate cloud using subsonic boundary conditions. Also, since at the time of particle formation the gas density is typically much smaller than the solid material, the velocity gained by the particles is very small relative to the gas

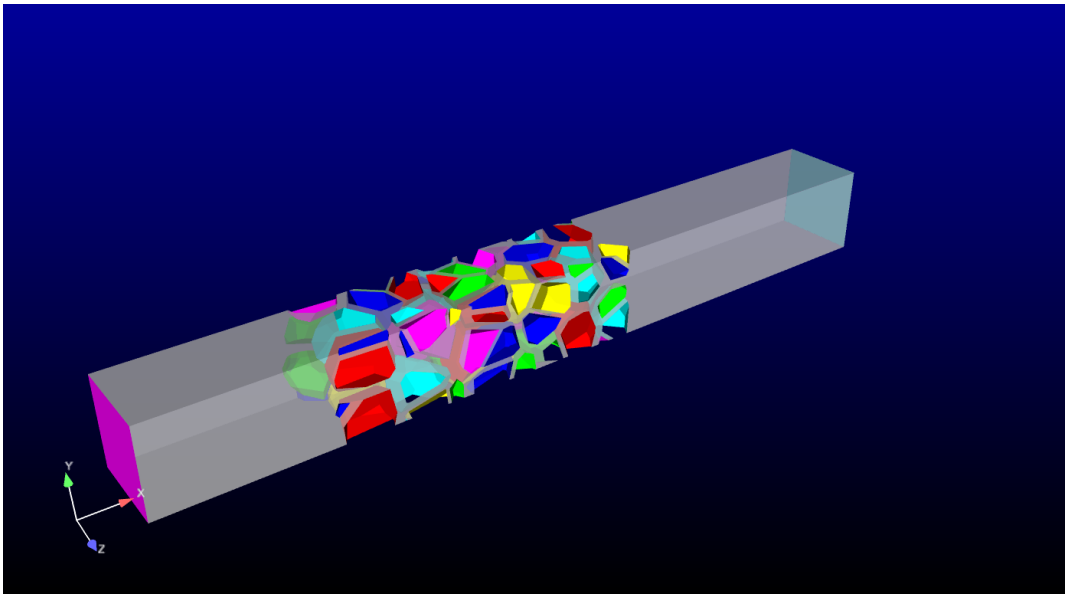

Figure 4: Configuration of soil fragments with highest particle volume fraction (57.8%)

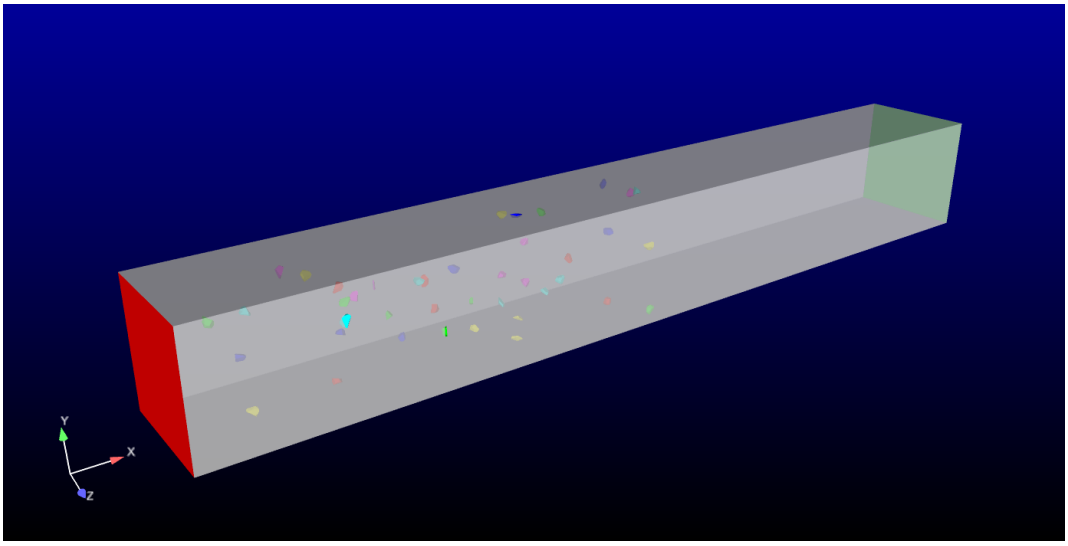

Figure 5: Configuration of soil fragments with lowest particle volume fraction (0.1%)

velocity. Therefore, it is reasonable to assume, for the purpose of developing drag laws, that the particles are stationary. While the particles will move, their movements will be over a much larger time scale than the time scale of the gas flow. A high temperature gas flows through soil fragments. The current model employed a gas modeled as an ideal gas with temperature of $2000K$. The inflow boundary condition was isentropic with total pressure of $10atm$. There were several number of pressure set up at outflow boundary, namely $2atm$, $3atm$, $4atm$, $5atm$ and $7atm$. Simulations from these different outflow pressure suggested that flow undergoes choking due to the blockage effect of soils, as shown in figure 6. Therefore, drags exerted on particles were not sensitive to outflow pressure except for those closest to the outflow boundary. This conclusion was also justified in the simulation results under different outflow pressures. Thus, we only chose the simulations with outflow boundary pressure of $5atm$ for construction of our drag database. The pressure distributions on the soil fragments under different particle volume fraction are demonstrated in figs 7 to 12. It is clear that the pressure change across the domain occupied by soil blocks decreases as the the flow becomes more dilute.

Two non-dimensional variables needed in the drag model are drag coefficient (C_d), Reynolds number based on particle size (Re_d). They are defined as :

$$C_d = \frac{2 * F_d}{Au^2} \tag{1}$$

$$Re_d = \frac{\rho(u - u_p)d}{\mu} \tag{2}$$

where F_d is the drag force exerted on soil fragments, while u and u_p denote the speed of gas and soil. As mentioned before, u_p is considered zero in our simulations. The density and dynamic viscosity of the gas are represented by ρ and μ respectively. The variable A represents the projected area of particle in the flow direction, while d represents the diameter of the particle. In our simulations, the shape of soil fragments was non-spherical, thus particle diameter, d, is defined by the volume-equivalent-sphere diameter or nominal diameter represented as $d = \sqrt[3]{6V/\pi}$ where V is the particle volume.

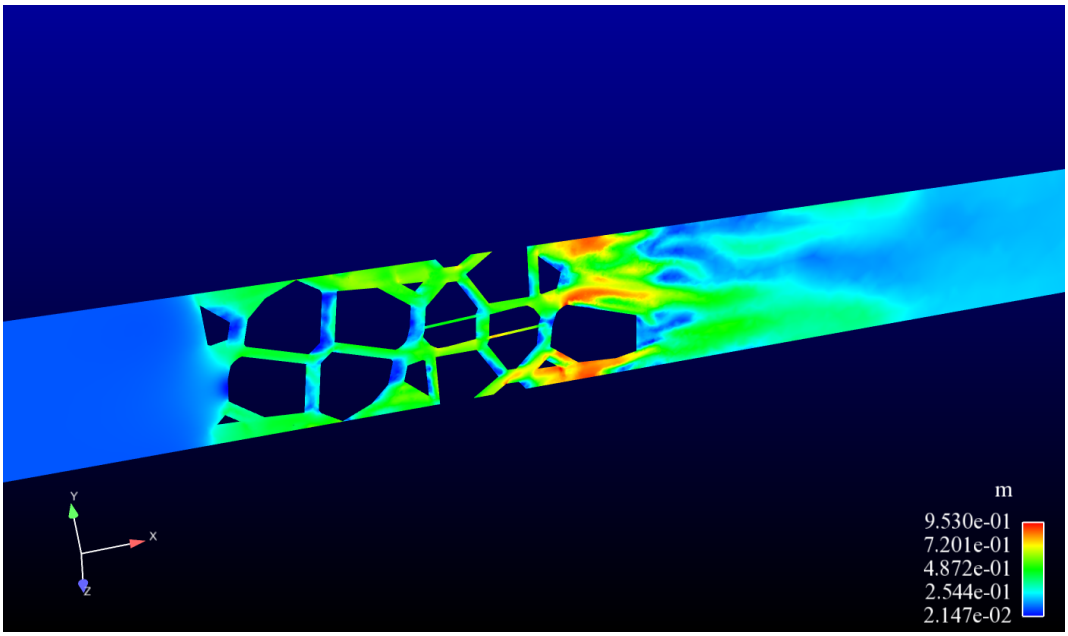

Figure 6: Mach number distribution at $z = 0$ cutting plane

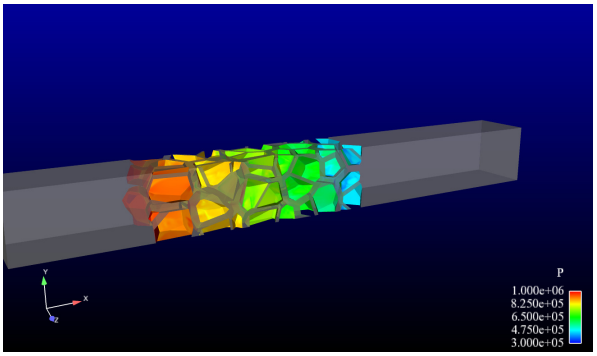

Figure 7: Pressure distribution on soil fragments for 57.8% particle volume fraction

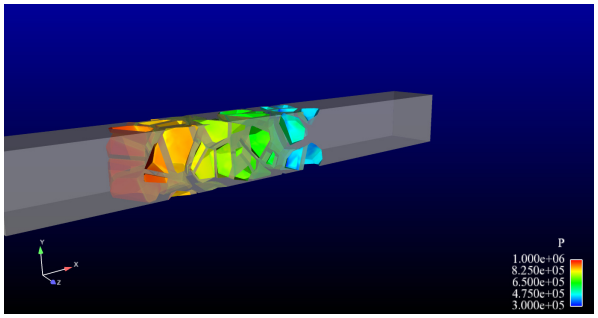

Figure 8: Pressure distribution on soil fragments for 51.2% particle volume fraction

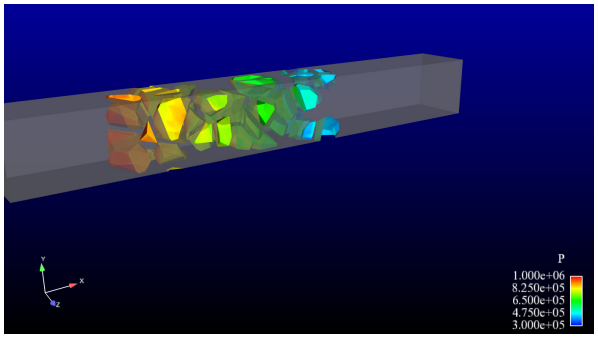

Figure 9: Pressure distribution on soil fragments for 29.6% particle volume fraction

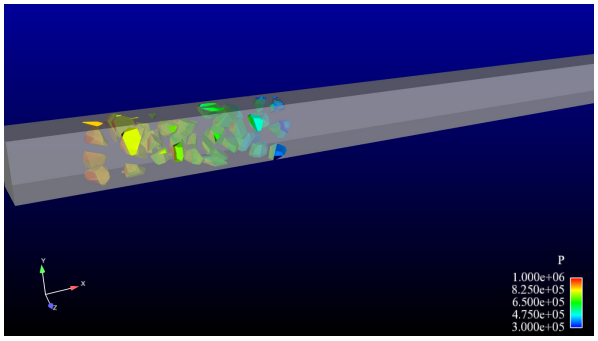

Figure 10: Pressure distribution on soil fragments for 12.5% particle volume fraction

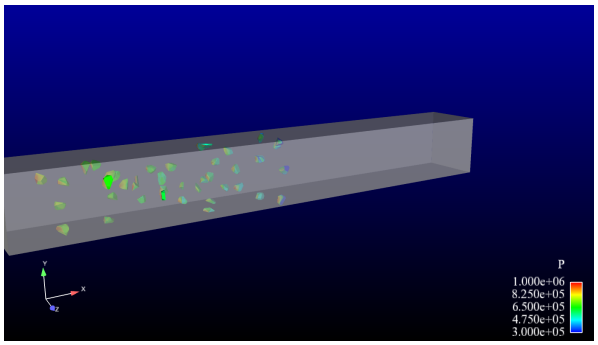

Figure 11: Pressure distribution on soil fragments for 8% particle volume fraction

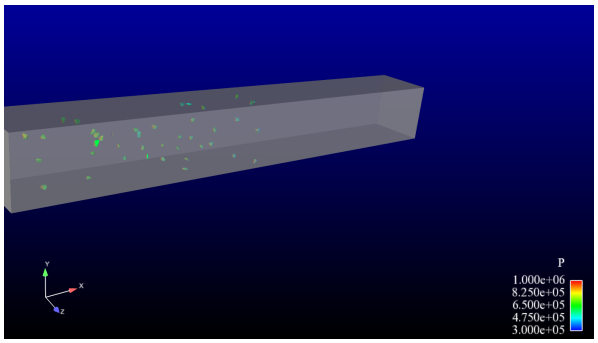

Figure 12: Pressure distribution on soil fragments for 0.1% particle volume fraction

Since there is a wide distribution of values of the variables in the simulation domain, it is important to define a sensible set of variables for nondimensionalization. Since in practice we will be utilizing this database to represent the integrated effects throughout a cell volume that is generally much larger than soil particulate sizes, we adopted values that result from integrations around the region of each particle in order to obtain values, such as fluid velocity and density, that are used for nondimensionalization. To perform this integration we implemented a tool that computes the volume-averaged local variables (e.g. u,μ,ρ) in the median volume around each soil fragment, defined as:

$$s = \frac{\sum s_i vol_i}{\sum vol_i} \tag{3}$$

where s stands for any median volume averaged variable, and vol is the volume of the cell. Index i represents the cell that within the median volume of the soil fragment. The median volume associated with soil fragment is all the cells that are closer to the given soil fragment than any others. It was observed that there were a significant amount of noises in the data around each soil fragment due to localized variability in the particle arrangement and shape. Therefor we determined to use averaged values over the computational domain to compute drag coefficients for the database. The averaged values of variables, such as drag force, velocity, diameter and other properties of soil, were obtained by averaging the corresponding information associated with each soil fragment excluding the parts whose median volumes extended all the way to the inflow or outflow boundaries, i.e. particles that were at the leading or trailing edges of the simulated particles.

Note that the drag force on soil fragment in the case of high particle volume fraction comes from the combination of the local effect of flow around the soil fragments and the global effect associated with the bulk pressure change due to the blockage presented by the large volume fraction. When particle volume fraction decreases, the pressure change across the computational domain decreases, thus the drag force becomes dominated by local inviscid and viscous effects. This distinction is important since in the context of a drag law, the mesh in the nominal CFD solution is much larger than the particle

size so the bulk effects of pressure gradient acting over the surface of the particles will be directly captured as an average behavior by the CFD solver, whereas local effects need to be provided by a phenomenological model. To obtain this distinction between average bulk effects resolved by the large scales and the small scale effects, we consider the effect of the bulk pressure gradient in these detailed particle-scale simulations. In order to characterize this local effect, we defined another drag coefficient, C_{dl}, that excludes the global pressure gradient, as follows

$$C_{dl} = \frac{2 * (F_d - F_{pg})}{Au^2} \tag{4}$$

where F_{pg} is the force due to the bulk pressure gradient. This bulk pressure gradient is computed by integrating pressure over the surface of median volume which excludes the particle local effect such as stagnation, and then by scaling the value to the area of corresponding soil fragment based on the ratio of the surface area of the soil fragment to the surface area of the median volume.

4 Database and Drag Model

The database of drag is presented in table 1. As mentioned previously, the values in the database are averaged over computational domain due to the large fluctuations in the data around each soil fragment. The magnitude of Reynolds number covers from 10^2 to 10^5, and particle volume fraction has a 2 order range of values. In the table, C_{dp} is the parameter based on the bulk pressure effect on particles, and defined as $C_{dp} = C_d - C_{dl}$. It shows that the contribution from bulk pressure gradient decreases as flow becomes more dilute due to less blockage effect from the expanding soil fragments. When the particle volume fraction approaches zero, the effect from bulk pressure gradient imposed on soils is negligible, and the drag force results from the local effect around soils.

We applied data regression to obtain local drag coefficient dependency on particle volume fraction and Reynolds number based on particle size, i.e. $C_{dl} = f(Re_d, \alpha)$. It is observed in table 1 that drag

coefficient based on the total drag force (C_d) increases monotonically with particle volume fraction, while local drag coefficient that excludes the bulk pressure term, C_{dl}, does not have monotonic behavior with particle volume fraction. However, the non-dimensional parameter that characterizes the bulk pressure gradient ($C_{dp} = C_d - C_{dl}$) demonstrates monotonic increase with particle volume fraction. Due to the lack of the monotone behavior of C_{dl}, we determined that a better strategy was to perform data regression on C_d and C_{dp} such that a more accurate fitting would be achieved. The model for the local drag coefficient (C_{dl}) was then computed by subtracting contribution due to the bulk pressure gradient (C_{dp}) from the total drag coefficient (C_d).

A data regression open-source software package, R-language (http://www.r-project.org/), which has been widely used in statistical community was adopted as our data analysis toolset. The new drag model should converge to a traditional drag law for isolated particles as particle volume fraction approaches to zero. One of the most widely used drag law for isolated spheres is the empirical equation of Clift and Gauvin. [Clift and Gauvin, 1970], which is valid for particle Reynolds number up to 3×10^5 and reads as:

$$C_{d0} = \frac{24}{Re_d}(1 + 0.15Re_d^{0.687}) + \frac{0.42}{1 + 4.25 \times 10^4 Re_d^{-1.16}} \tag{5}$$

where C_{d0} stands for the drag coefficient when the particle volume fraction is zero. In this study, two additional effects needs to be taken into account in the drag law of isolated particles, namely compressibility effect and non-spherical particle effect . When the particle Reynolds number is not too low ($Re_d > 45$), the formation of shock waves on the particles and attendant wave drag increase the drag force acting on the particles. This compressibility effect becomes significant when Mach number reaches 0.6, which is the critical Mach number. We adopted the drag model developed by Loth [Loth, 2008] for the correction of the Mach number effect:

$$C_{d0} = \frac{24}{Re_d}(1 + 0.15Re_d^{0.687}) * (1.0 - \frac{0.258 * CM}{1.0 + 514 * GM}) + \frac{0.42 * CM}{1 + 4.25 \times 10^4 * GM * Re_d^{-1.16}} \tag{6}$$

Table 1: Drag coefficients vs Reynolds number (Re_d) and volume fraction (α) under different particle sizes

	C_d	C_{dl}	C_d -C_{dl}	Re_d	α
	7.798	3.239	4.559	148.9	0.579
	4.600	2.190	2.410	188.9	0.512
$d \sim 0.1mm$	1.950	1.298	0.652	333.0	0.296
	1.454	1.195	0.259	449.9	0.125
	0.973	0.950	0.023	719.7	0.008
	0.909	0.903	0.006	834.0	0.001
	2.930	1.167	1.763	710.3	0.579
	2.284	1.041	1.243	787.6	0.512
$d \sim 0.3mm$	1.532	0.992	0.540	1125.4	0.296
	1.317	1.070	0.247	1373.0	0.125
	0.942	0.919	0.023	2161.0	0.008
	0.853	0.847	0.006	2502.1	0.001
	1.897	0.712	1.185	2883.6	0.579
	1.685	0.745	0.940	3028.3	0.512
$d \sim 1mm$	1.440	0.920	0.520	3830.2	0.296
	1.293	1.045	0.248	4578.5	0.125
	0.953	0.930	0.023	7154.3	0.008
	0.860	0.854	0.006	8346.7	0.001
	1.685	0.613	1.072	9104.4	0.579
	1.515	0.660	0.855	9576.1	0.512
$d \sim 3mm$	1.391	0.869	0.522	11602.8	0.296
	1.300	1.051	0.249	13547.7	0.125
	0.938	0.916	0.022	21514.5	0.008
	0.822	0.816	0.006	24971.0	0.001
	1.567	0.560	1.007	31335.5	0.579
	1.511	0.691	0.820	33146.0	0.512
$d \sim 1cm$	1.369	0.853	0.516	38640.9	0.296
	1.320	1.072	0.248	44995.2	0.125
	0.974	0.951	0.023	71603.3	0.008
	0.859	0.854	0.005	83425.2	0.001

where CM and GM are function of Mach number, M, and are defined as:

$$CM = \frac{5}{3} * tanh(3.0 * log(M + 0.1)) \quad if M \leq 1.45 \tag{7}$$

$$CM = 2.044 + 0.2 * exp(-1.8 * (log(\frac{M}{2}))^2) \quad if M > 1.45 \tag{8}$$

$$GM = 1.0 - 1.525 * M^4 \quad if M \leq 0.89 \tag{9}$$

$$GM = 0.0002 + 0.0008 * tanh(12.77 * (M - 2.02)) \quad if M > 0.89 \tag{10}$$

For non-spherical particles in an infinite medium, it is generally recognized that a shape factor must be included in the expression of drag coefficient. Shape factor of Tran-Cong et. al [Tran-Cong et al., 2004] was utilized to modify the drag model as follows:

$$C_{da} = C_{d0} * (\frac{d_A}{d})^2 \tag{11}$$

where C_{da} represents the drag coefficient with consideration of particle irregularity, and d is the volume-equivalent-sphere diameter defined earlier. The surface-equivalent-sphere diameter, d_A, is written as $d_A = \sqrt{4A_p/\pi}$ where A_p is the projected area of the particle. The ratio d_A/d is used as the dimensionless shape factor to account for the non-spherical effect of particles on drag force.

Using muti-variable nonlinear data regression technique in R-language, the new drag models with particle volume fraction being a dependency variable were obtained:

$$C_d = C_{da} + A1 * \alpha * (1.0 + \frac{D1}{Re_d^{c1}})^4 + B1 * \alpha * (1.0 + \frac{D1}{Re_d^{c1}}) \tag{12}$$

$$C_{dl} = C_{da} + A1 * \alpha * (1.0 + \frac{D1}{Re_d^{c1}})^4 + B1 * \alpha * (1.0 + \frac{D1}{Re_d^{c1}}) - A2 * \alpha * (1.0 + \frac{D2}{{Re_d}^{c2}})^6 - B2 * \alpha * (1.0 + \frac{B2}{{Re_d}^{c2}}) \tag{13}$$

where fitting coefficients are given by $A1 = 0.5048, B1 = 0.9858, c1 = 0.5707, D1 = 34.8$ for the total drag coefficient, C_d, and $A2 = 1.876, B2 = 1.4285, c2 = 0.4775, D2 = 9.4926$ for the pressure drag coefficient, C_{dp}. It is obvious that the drag models become conventional drag law of isolated particles when particle volume fraction is zero. The drag models show that drag force increases with particle volume fraction,and the steepest increase happens at small α and Re_d, which was evaluated by the higher power in the model functions. Figures 13 and 14 demonstrate comparison between numerical data and the results from our new drag models based on total drag and local drag force, respectively. In the figures, the surfaces defined by the green grids represent the data from particle-scale simulations while the surfaces from the drag models are shown in blue. Tables 2 and 3 show comparison of drag coefficients from database and proposed model. The relative error is defined as the absolute value of the difference between numerical data and result from the model divided by numerical data. It is seen that the fitting errors at low end of particle volume fraction are relatively higher with our models due to an over-prediction compared with the database. The square root of sum of square of each relative error is 9.4% for C_d, and 10.2% for C_{dl}. These results indicate that the proposed drag models provide satisfactory agreement with data from particle-scale simulations.

Before we close this section, it is helpful to discuss some issues not concerned in the development of our drag model so that we understand some of the limitations. In our particle-scale simulations in which soil clouds uniformly expanding in the domain, it is assumed that soil fragments remains their orientations during the simulations while in reality the soil pieces might rotate due to the moment imposed on them. The ignorance of the particle rotation could cause the inaccurate prediction of the drag force. However, the complexities involved in rotation and spinning of the soil fragments would make the development of drag model intractable in the current stage, and our present drag model mainly reflect the blockage effect on multiphase flows. Since the time scale of blast detonation is very small, it is reasonable to treat soil fragments irrotational. Another factor not considered in the model is compressibility effect under high particle volume fraction. We assume that flow is choked and Mach number does not change significantly over the simulation domain. In the future study, database will

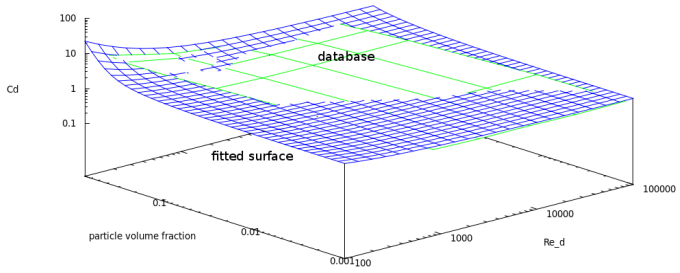

Figure 13: Comparison of variation of total drag coefficient (C_d) with particle volume fraction and Reynolds number between numerical data and proposed model

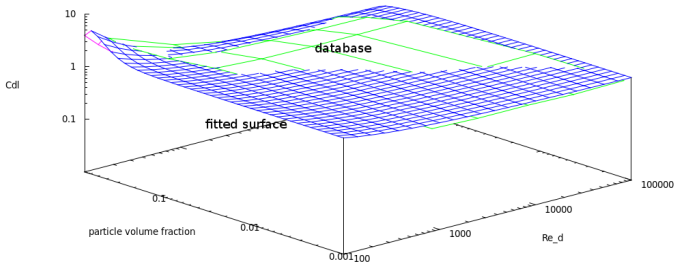

Figure 14: Comparison of variation of local drag coefficient (C_{dl}) with particle volume fraction and Reynolds number between numerical data and proposed model

Table 2: Comparison of total drag coefficients (C_d) between database and model results

C_d from database	C_d from the model	relative error	volume fraction
7.798	7.753	0.6 %	0.579
4.600	4.729	2.8 %	0.512
1.950	1.986	1.9 %	0.296
1.454	1.427	1.9 %	0.125
0.973	1.121	15.2 %	0.008
0.909	1.092	20.1 %	0.001
2.930	2.769	5.5 %	0.579
2.284	2.335	2.2 %	0.512
1.532	1.564	2.1 %	0.296
1.317	1.237	6.1 %	0.125
0.942	1.023	8.6 %	0.008
0.853	1.004	17.8 %	0.001
1.897	1.975	4.1 %	0.579
1.685	1.796	6.6 %	0.512
1.440	1.375	4.5 %	0.296
1.293	1.131	12.5 %	0.125
0.953	0.964	1.2 %	0.008
0.860	0.950	10.5 %	0.001
1.685	1.739	3.2 %	0.579
1.515	1.611	6.4 %	0.512
1.391	1.285	7.6 %	0.296
1.300	1.075	17.3 %	0.125
0.938	0.930	0.9 %	0.008
0.822	0.919	11.7 %	0.001
1.567	1.618	3.3 %	0.579
1.511	1.512	0.0 %	0.512
1.369	1.230	10.2 %	0.296
1.320	1.038	21.4 %	0.125
0.974	0.906	7.1 %	0.008
0.859	0.896	4.3 %	0.001

Table 3: Comparison of local drag coefficients (C_{dl}) between database and model results

C_{dl} from database	C_{dl} from the model	relative error	volume fraction
3.239	3.189	1.5%	0.579
2.190	2.364	8.0%	0.512
1.298	1.292	0.5%	0.296
1.195	1.157	3.2%	0.125
0.950	1.104	16.2%	0.008
0.903	1.090	20.6%	0.001
1.167	1.040	10.9%	0.579
1.041	1.069	2.7%	0.512
0.992	0.994	0.2%	0.296
1.070	1.005	6.1%	0.125
0.919	1.009	9.7%	0.008
0.847	1.003	18.3%	0.001
0.712	0.750	5.4%	0.579
0.745	0.810	8.7%	0.512
0.920	0.871	5.4%	0.296
1.045	0.922	11.8%	0.125
0.930	0.951	2.3%	0.008
0.854	0.948	11.0%	0.001
0.613	0.671	9.5%	0.579
0.660	0.726	10.0%	0.512
0.869	0.814	6.3%	0.296
1.051	0.879	16.3%	0.125
0.916	0.917	0.2%	0.008
0.816	0.917	12.3%	0.001
0.560	0.631	12.6%	0.579
0.691	0.682	1.3%	0.512
0.853	0.779	8.7%	0.296
1.072	0.849	20.7%	0.125
0.951	0.894	6.0%	0.008
0.854	0.894	4.8%	0.001

include Mach number, and drag coefficient on soil fragments will be a function of Mach number besides two variables in the present work.

5 Summary and concluding remarks

The objective of this study was to develop a phenomenological drag model to characterize the momentum coupling between the detonation gas and soil fragments when the soil initially breaks into a dense particulate cloud. We conducted a series of numerical simulations on the scale of soil fragment by only considering a small region occupied by a mixture of blast gas and soil fragments. Voronoi graph was adopted to model the geometry of soil breaking. Different expansion ratios between the Voronoi points were applied to form six soil volume fractions, covering the cases with densely packed soil cloud to the situations with dilutely distributed soil fragments. Five different particle sizes were considered under each soil volume fraction. In the simulations, only one value of pressure was imposed at the outflow boundary since the flow underwent choking due to the blockage of the soil. A drag database was constructed based on the drag force collected from the particle-scale simulations. A new drag law was developed using data regression technique to characterize the dependency of the drag force exerted on particles as a function of particle volume fraction and Reynolds number based on particle size. The irregularity of the particles was also considered in the drag model. The proposed drag law provides satisfactory representations of the simulation data, and converge to traditional drag model for isolated particles when the particle volume fraction approaches to zero.

6 Acknowledgments

This work is supported by the U.S.Army TACOM Life Cycle Command under Contract No.W56HZV-08-C-0236, through a subcontract with Mississippi State University, and was performed for the Simulation Based Reliability and Safety (SimBRS) research program.

References

[Clift and Gauvin, 1970] Clift, R. and Gauvin, W. H. (1970). The motion of particles in turbulent gas streams. *Proc. Chemeca'70*, 14(1).

[Crowe, 1998] Crowe, C. T. (1998). *Multiphase Flows with Droplets and Particles*. CRC Press.

[Gaither et al., 2000] Gaither, A., Marcum, D., and Mitchell, B. (2000). Solidmesh: A solid modeling approach to unstructured grid generation. In *Proceedings of the 7th International Conference on Numerical Grid Generation in CFS*.

[Gidaspow, 1994] Gidaspow, D. (1994). *Multiphase Flows with Fluidization*. Academic Press.

[Loth, 2008] Loth, E. (2008). Compressibility and rarefaction effects on drag of a spherical particle. *AIAA*, 46(9):2219–2228.

[Tran-Cong et al., 2004] Tran-Cong, S., gay, M., and Michaelides, E. (2004). Drag coefficients of irregularly shaped particles. *Powder Technology*, 139:21–32.